POROSITY AND DRAG DETERMINATION OF A SINGLE-ROW VEGETATIVE BARRIER (*MACLURA POMIFERA*)

H. B. Gonzales, M. E. Casada, L. J. Hagen,
J. Tatarko, R. G. Maghirang, C. J. Barden

ABSTRACT. *Deciduous trees of the species* Maclura pomifera *(Osage orange) are commonly established as vegetative barriers for wind erosion control throughout the U.S. Great Plains. Because there is no previous research on the aerodynamic effectiveness of these vegetative barriers during different seasons (leaf-on and leaf-off conditions), this study focused on determining the porosity and drag characteristics of this tree species. Digital image analyses were used to determine optical porosities that were then correlated with barrier drag coefficients. Images were taken in the field during calm wind conditions when the sunlight was suitable for digital imaging. Wind speeds were measured at different heights for a single-row Osage orange barrier using cup anemometers. Two anemometer towers were positioned relative to the barrier. One was located windward at 10H distance from the barrier; the other was located leeward and was movable to distances of 1H, 2H, 4H, 7H, 10H, 12H, 15H, and 20H from the barrier, where H is the average barrier height. The wind speeds measured in the field ranged from 4 to 7 m s^{-1}, with lower wind speeds encountered during the leaf-off condition. As expected, wind speed reductions were greater for the leaf-on condition and ranged from 40% to 80% at 1H from the barrier, while the reduction was 20% to 38% for the leaf-off condition. The crown portion of the barrier was found to be responsible for much of the reduction. Mean values of the drag coefficient were 1.3 for the leaf-on condition, decreasing to 0.9 for the leaf-off condition of the Osage orange barrier, which corresponded to mean optical porosities of 20% and 61%, respectively.*

Keywords. *Drag coefficient, Image analysis, Osage orange, Porosity, Vegetative barrier, Wind erosion.*

Arid and windy regions, such as the U.S. Great Plains, are susceptible to wind erosion. Methods such as conservation tillage, strip cropping, and vegetative barriers have been implemented to minimize wind erosion effects. Farmers often use vegetative barriers (also called windbreaks or shelterbelts) to shelter leeward fields from wind and prevent wind erosion. Other benefits of vegetative barriers include changing the microclimate of soils (Cleugh, 1998; Campi et al., 2009), increased crop yield (Kort, 1988; Sun and Dickinson, 1997; Sudmeyer et al., 2002), crop protection (Kort, 1988; Bird et al., 1992), restoration of soil fertility (Sudhishri et al., 2008), livestock protection (Gregory, 1995; Ffolliott, 1998), increased livestock performance (Mader et al., 1999), and aesthetic and wildlife benefits (Burel and Baudry, 1995; Grala et al., 2010).

The effectiveness of a vegetative barrier is commonly measured by its sheltering efficiency leeward of the barrier via reduced wind speed (Kozmar et al., 2012). This effectiveness is dependent on factors such as the tree species, shape, height, length, width, orientation, canopy density, and porosity (Brandle et al., 2004; Cornelis and Gabriels, 2005; Koh et al., 2014). Porosity is an essential parameter that defines the relative sheltering efficiency of vegetative barriers (Hagen and Skidmore, 1971). Solid barriers promote excessive recirculation (zones of low wind speed and increased turbulence) windward and leeward of the barrier (Billman Stunder and Arya, 1988). Porous barriers minimize recirculation, provided that the porosities are greater than about 20% (Hagen and Skidmore, 1971; Wilson, 1987; Cornelis and Gabriels, 2005). Excessively low porosity induces fast recovery of leeward wind speed, potentially promoting increased turbulence via recirculation, similar to a solid barrier, but excessively high porosity is undesirable because it does not effectively shelter the leeward side of the vegetative barrier.

Both the aerodynamic (α_p) and optical (β_p) porosities of a vegetative barrier can be defined. Aerodynamic porosity (volumetric porosity) is the true porosity, which considers the complete three-dimensionality of the barrier, but it is dif-

Submitted for review in March 2017 as manuscript number PAFS 12338; approved for publication by the Plant, Animal, & Facility Systems Community of ASABE in December 2017.

Mention of company or trade names is for description only and does not imply endorsement by the USDA. The USDA is an equal opportunity provider and employer.

The authors are **Howell B. Gonzales,** Postdoctoral Fellow, Department of Earth and Environmental Sciences, Temple University, Philadelphia, Pennsylvania; **Mark E. Casada,** Research Agricultural Engineer, USDA-ARS Center for Grain and Animal Health Research, Manhattan, Kansas; **Lawrence J. Hagen,** Research Agricultural Engineer (retired), USDA-ARS Stored Product Insect and Engineering Research Unit, Manhattan, Kansas; **John Tatarko,** Soil Scientist, USDA Rangeland Resources and Systems Research Unit, Fort Collins, Colorado; **Ronaldo G. Maghirang,** Professor, Department of Biological and Agricultural Engineering, and **Charles J. Barden,** Professor, Department of Horticulture and Natural Resources, Kansas State University, Manhattan, Kansas. **Corresponding author:** Mark E. Casada, 1515 College Ave., Manhattan, KS 66502; phone: 785-776-2758; e-mail: mark.casada@ars.usda.gov.

ficult to compute. According to Heisler and DeWalle (1988), α_p can be approximated from β_p for narrow and thin vegetative barriers. Thus, optical porosity is a two-dimensional approximation of the true porosity. A thin vegetative barrier is defined as a vegetative barrier across which the wind variation is negligible due to the small ratio of the vegetative barrier's width to its height (Wilson, 2005; Bouvet et al., 2007). Guan et al. (2003) gave the following equation for α_p:

$$\alpha_p = \frac{\int_0^H \overline{u}(z)\,dz}{\int_0^H \overline{u}_0(z)\,dz} \quad (1)$$

where H is the height of the barrier (m), $\overline{u}(z)$ is the leeward wind speed (bleed wind speed) (m s^{-1}), and $\overline{u}_0(z)$ is the mean windward (or approaching) wind speed (m s^{-1}). Optical porosity is obtained from the following equation:

$$\beta_p = \frac{(Background\ area)}{(Total\ area)} \quad (2)$$

Guan et al. (2003) obtained the background area (representing the gaps outside the areas occupied by the tree, which includes the leaves, branches, and trunk) from image analysis of digitized photographs. They used a systematic approach of taking photographs of tree sections in accordance with guidelines proposed by Loeffler et al. (1992). Although β_p is convenient to use because it does not require wind measurement, a relationship between α_p and β_p is necessary, especially for deciduous trees that experience porosity variations throughout the year.

Accurate choice of barrier species is essential for alleviating the effects of wind erosion (Hagen and Skidmore, 1971; Steffens et al., 2012). Although numerous studies of vegetative barriers have been conducted, the structural complexity of various tree species has led to limited research on the types of vegetative barriers that have been established on the perimeters of agricultural lands in Kansas. Barrier porosity is specific to the tree type (Hagen and Skidmore, 1971; Wang and Takle, 1996; Koh et al., 2014) due to the variations in shape, height, and porosity dictated by various foliage structures. Osage orange (*Maclura pomifera*), or hedge apple, which is commonly used for vegetative barriers in Kansas, is a tree species that sheds its leaves during the dormant season (deciduous). This tree can grow to a height of 8 to 15 m with round, bumpy fruit that measures 7 to 16 cm in diameter. Although use of Osage orange as a vegetative barrier is prevalent on agricultural lands in Kansas, no quantitative information is available on the aerodynamic properties of Osage orange in both the leaf-on and leaf-off conditions. In addition to defining the seasonal changes that this tree species experiences, a need exists to define the aerodynamic parameters that characterize the effectiveness of Osage orange as a shelter for leeward crops and soil during its two leaf conditions (leaf-on and leaf-off). Specific objectives of this study were to:

1. Determine the optical porosity of an Osage orange barrier section using image analysis.
2. Determine the aerodynamic porosity and drag coefficients of Osage orange during leaf-on and leaf-off conditions using wind profile measurements.
3. Measure the effects of barrier leaf condition on wind speed reduction.

Materials and Methods

Site Description

This research was conducted from October to December 2013 at a farm near Riley, Kansas (39° 18′ 49.1″ N, 96° 54′ 29.2″ W) where Osage orange was used as a vegetative barrier (fig. 1). The site was chosen based on the following criteria proposed by Loeffler et al. (1992): (1) flat terrain to avoid topographical effects on wind speed patterns close to the vegetative barrier; (2) absence of obstructions, such as buildings, in the vicinity to avoid adverse effects on wind speed patterns along the vegetative barrier; (3) similar vegetation height on both sides of the barrier to maintain constant surface roughness; and (4) a minimum length:height ratio of 10:1 to avoid edge and vortex effects at the ends of the vegetative barrier.

The chosen field (fig. 1) was almost completely flat along the measured wind direction (0% slope on the south and <1% on the north side), and wind measurements were taken using cup anemometers (fig. 3). The field, with an east-west vegetative barrier separating it in the middle, was located at an elevation of 508 m and had a length of 300 m (north to south) and width of 200 m (east to west). Field crops grown in rotation included winter wheat (*Triticum aestivum*), corn (*Zea mays*), and sorghum (*Sorghum bicolor*). In addition to the vegetative barrier within the field, no-till management was employed to minimize the effects of wind erosion and improve production. The average (of ten trees) measured tree height (H) was 8.5 ±0.6 m, which was used as a basis for data analysis. During field measurements for the leaf-on condition of the Osage orange barrier (October), the west side of the leeward field was planted to winter wheat (0.1 to 0.15 m height), so wind speeds were determined at the eastern portion of the leeward field, where soybean stubble was present at the time (freshly harvested soybean, about 0.1 m height). The windward field was bare at the time of sampling, with sorghum stubble (~0.1 m height). During the leaf-off condition (December), the leeward field had the same crop configuration as during the leaf-on measurements. Figure 2 shows the leaf-on and leaf-off conditions during measurements.

Prevailing wind directions for the field site are south-southwest for the summer and north-northwest for the winter. Data were collected in the presence of a direct south wind or a south-southwest wind for both tests (summer and fall).

Wind Profiles

Two towers were positioned, with one on each side of the vegetative barrier. Given the prevailing winds at the time of measurement, the north side was the leeward side and the south side was the windward side. The leeward tower was a mobile tower placed at distances of 1H, 2H, 4H, 7H, 10H,

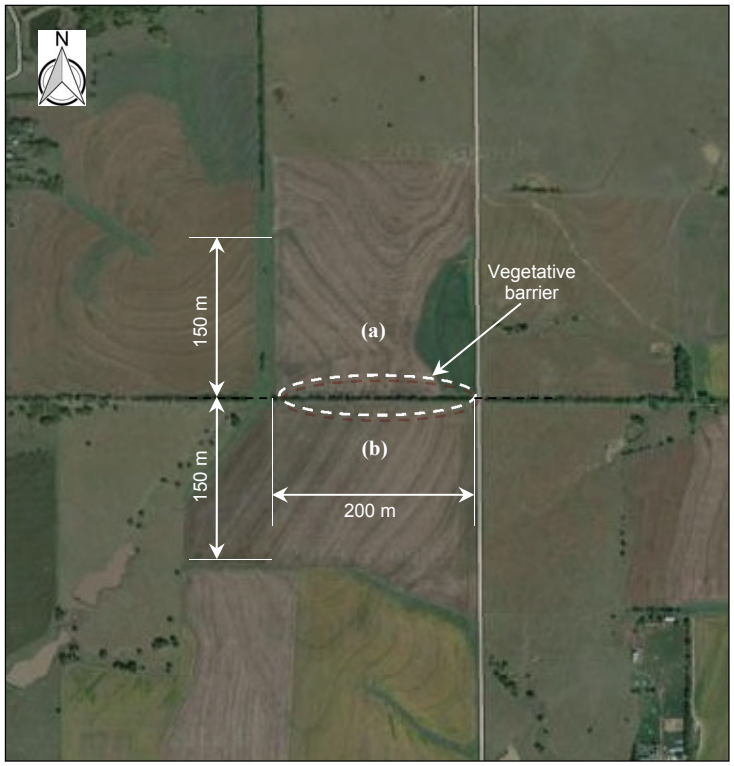

Figure 1. Aerial view of field site (via Google Maps, 2013): (a) north (leeward) side and (b) south (windward) side.

15*H*, and 20*H* from the chosen section of the barrier, based on distances used by Stredova et al. (2012). The distances of 15*H* and 20*H* were included to determine the leeward extent of wind speed recovery. This tower was equipped with cup anemometers (Sierra Misco 1005 DC, NovaLynx Corp., Grass Valley, Cal.) installed on mounting arms along the height of the tower at heights of 1.5, 3.35, 4.9, 6.4, 8.2, and 15 m above the ground (fig. 3). The windward tower was a stationary tower located 85 m windward from the barrier. The windward tower was equipped with cup anemometers at the same heights as the leeward tower and included an additional cup anemometer at 18 m above the ground. The topmost anemometers at 15 m (leeward) and 18 m (windward) heights were only used for collecting wind speeds above the barrier height that were necessary for computation of the approach flow and were not used in comparisons of wind speeds within the barrier. The wind speed reduction and optical porosity computations used only the bottom five anemometers because they were representative of heights within the Osage orange barrier, as shown in figure 3.

The anemometer heights in the field were similar to the heights used by Sellier et al. (2008). Wind profiles were recorded continuously (1 s intervals) for 10 min and were time-averaged at 1 min intervals and at a total time of 10 min. The measurements were replicated three times for 10 min each in consecutive increments at the windward location as well as at each distance to the leeward of the vegetative barrier. Each set of cup anemometers on a tower (six leeward and seven windward) was connected to a USB data acquisition (DAQ) board (model 2408, Measurement Computing Corp., Norton, Mass.) that was connected to a laptop running LabView software (LabView 2012, Professional Edition, National Instruments, Austin, Tex.) to monitor and record real-time wind speed data. The DAQ board had 16 single-ended (8 differential) analog inputs and 24-bit resolution for voltage measurements at up to 1000 samples per second, which is useful for multiple simultaneous measurements and for recording instantaneous data.

Calibration of Anemometers

Prior to mounting on the towers, the cup anemometers were calibrated to wind speeds measured with pitot-static tubes in the outdoor wind tunnel at the USDA-ARS Center for Grain and Animal Health Research in Manhattan, Kansas. The pitot tubes were attached to pressure transducers calibrated using surgical syringes and an inclined manometer air filter gauge (Series 250-AF, Dwyer Instruments, Michigan City, Ind.) to ensure stable pressure and voltage readouts during measurements. Data were recorded via a LabView program (LabView Student, ver. 2012, National Instruments, Austin, Tex.). The anemometers were tested in the wind tunnel through a range of wind speeds (2 to 15 m s^{-1}). They were tested individually to avoid affecting the recorded free-stream wind speed, which occurs if anemometers are tested side by side. Voltage corresponding to the degree of spin (i.e., voltage ranging from 1.5 to 3.3 V, corresponding to 310 to 630 rpm) for each cup anemometer was the basis for calibration.

Porosity Determination

Optical and aerodynamic porosity measurements were compared. Because many methods for determining optical porosity are available, we evaluated two alternate methods. To estimate β_p, the two image analysis methods were both

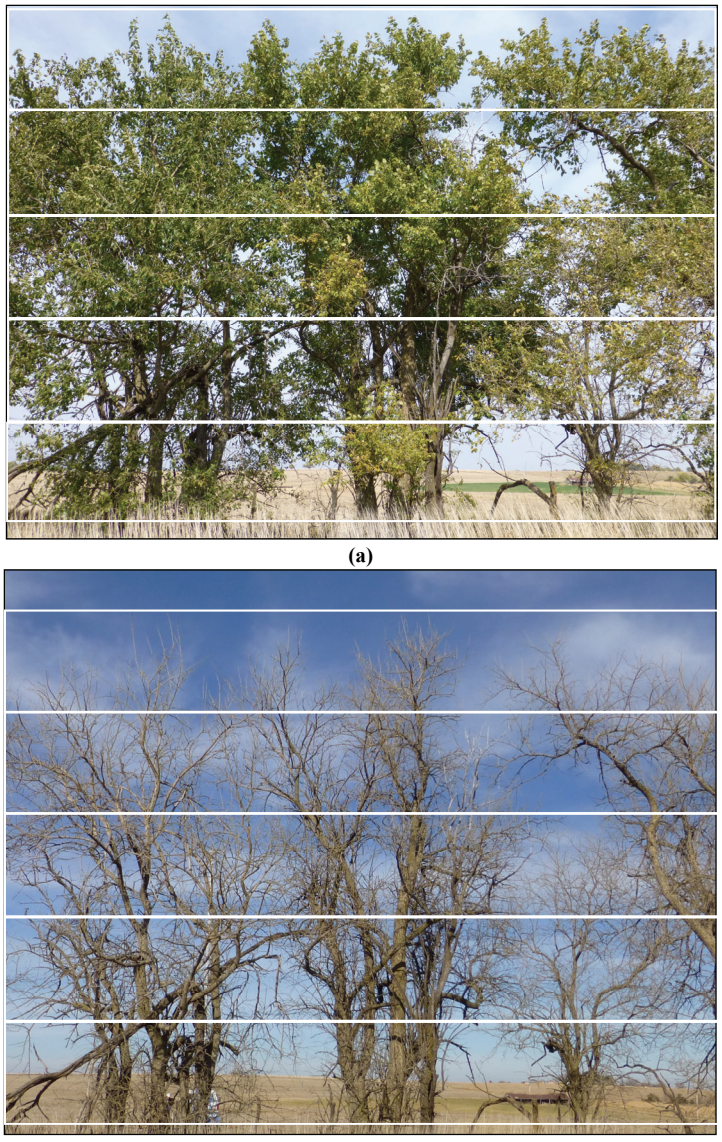

Figure 2. (a) Leaf-on and (b) leaf-off conditions tested for the Osage orange barrier showing five sections (separated by white lines) used for anemometer heights for porosity computations.

software products (SigmaScan Pro and MATLAB), and porosity values were compared for the leaf-on and leaf-off conditions of the Osage orange tree barrier. The two methods represent two different approaches: MATLAB uses a binary image approach, while SigmaScan Pro evaluates color images of the vegetative barrier. Digital images of a section of trees were captured using a Panasonic Lumix ZS20 camera with the lens at its 4.3 mm wide-angle setting (24 mm equivalent for 35 mm equivalent focal length) using a 14.1 megapixel 1/2.33″ type (6.2 mm × 4.5 mm image area) metal oxide semiconductor (MOS) sensor. Images of trees were taken one tree height away from the barrier in accordance with Kenney's (1987) guidelines and during calm (≤0.5 m s^{-1}) conditions. Following Zhu (2008), all images were taken in the absence of excessive brightness (12:00 p.m. to 1:00 p.m.), which could have increased the reflection from tree elements and thus promoted overexposure and unbalanced color in the images. The images considered for β_p computation were cropped from the ground to the apex of the Osage orange crown, similar to the method of Vigiak et al. (2003).

Figure 4 shows examples of digital image analysis using the two approaches: grayscale analysis and RGB (color) analysis. SigmaScan Pro was used to analyze digital images of true RGB color and determine the optical porosity value. The total area, determined to be the total number of pixels in the original image, and the background area were obtained from the difference between the total area pixels in the original image and the foreground area pixels. SigmaScan Pro identified foreground pixels after the user identified a representative pixel color for the foreground, which then served as the threshold pixel value. Thresholding was done by selecting a portion of the foreground (i.e., branches and leaves) and determining the value of a foreground pixel. This value was then taken as the threshold value to separate the foreground (tree) from the background (empty space). The selected object and other objects that exceeded the threshold

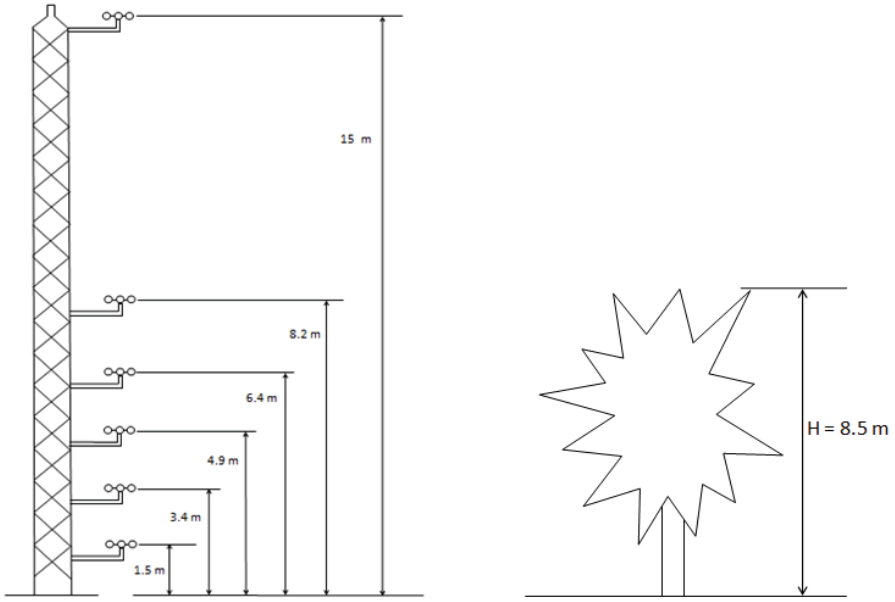

Figure 3. Schematic of the cup anemometers on the windward and leeward towers relative to the barrier height. The windward tower had an additional anemometer at 18 m height. Wind direction is perpendicular to the illustration of the tower.

pixel value were then filled with red color. If some portions of the original image were not separated from the background, further separation was done by continuously identifying objects to be included as foreground. Foreground selection often depends on the specific image (e.g., the presence of small branches greatly affects the threshold selection). Optical porosity was then calculated from the total foreground and total background areas (pixels) within the canopy.

In contrast, the MATLAB image analysis toolbox was used to convert the original image to grayscale and then to a binary image with specific numbers of pixels that defined the total area, background area, and foreground area. Finally, β_p was computed from these binary image pixel numbers.

Computation of α_p was based on the ratio of the mean leeward wind speed (mean of all 10 min bleed wind speeds at five heights, measured 1 m away from the barrier) to the mean windward wind speed (Guan et al., 2003; Bitog et al., 2011). For thin (single row) vegetative barriers, Heisler and DeWalle (1988) stated that α_p and β_p can approximate each other. Discrepancies between α_p and β_p occur due to inherent porosities and obscuration of light by leaves and branches (Grant and Nickling, 1998). In a field setting, wind speeds vary from the ground surface upward; therefore, the values of α_p also vary depending on the selected H value (H = 8.5 m for this study).

VEGETATIVE BARRIER DRAG COEFFICIENT

Based on measured values of wind speed, vegetative barrier drag is measured as the amount of resistance the trees offer to the incoming airflow (windward air) using a drag coefficient (C_D). Raine and Stevenson (1977) stated that changes in the airflow through a vegetative barrier are described by momentum shifts within the barrier as the barrier resists the incoming airflow. From the available literature, C_D can be computed as the ratio of wind load to the dynamic force windward of the barrier (Cullen, 2005; Koizumi et al., 2010; Bitog et al., 2011). For field conditions, the method of Hagen and Skidmore (1971), which was based on Woodruff et al. (1963), was adopted due to its simplicity and applicability, and the drag coefficient was estimated using the following equation:

$$C_D = \frac{2D_b}{\left(\rho_{air}\bar{u}^2 H\right)} \tag{3}$$

where D_b is the drag force per unit length of the vegetative barrier (kg s^{-2}), H is the vegetative barrier height (m), ρ_{air} is the air density (kg m^{-3}), and $\bar{u}$ is the mean windward wind speed over the wake depth (m s^{-1}).

Wake depth is the vertical distance at which the windward wind speed is equal to the leeward wind speed. Drag force was obtained using the difference in momentum transfer between the windward and leeward sides of the barrier, as explained by Woodruff et al. (1963) and defined by the following equation:

$$D_b + D_g = \int_0^S \left[\left(P_{up} + \frac{1}{2}\rho_{air}u_{up}^2\right) - \left(P_{down} + \frac{1}{2}\rho_{air}u_{down}^2\right)\right] dz \tag{4}$$

where D_b is the drag force of the barrier (kg s^{-2}), D_g is the drag force of the ground (kg s^{-2}), z is the vertical distance along the barrier height (m), P_{up} and P_{down} are windward and leeward pressure values (kg m^{-1} s^{-2}), and u_{up} and u_{down} are windward and leeward wind speeds (m s^{-1}).

Drag coefficient was calculated with a simplified equation derived by Hagen and Skidmore (1971), which neglected pressure effects by assuming the ground drag was negligible compared to the barrier drag (eq. 5):

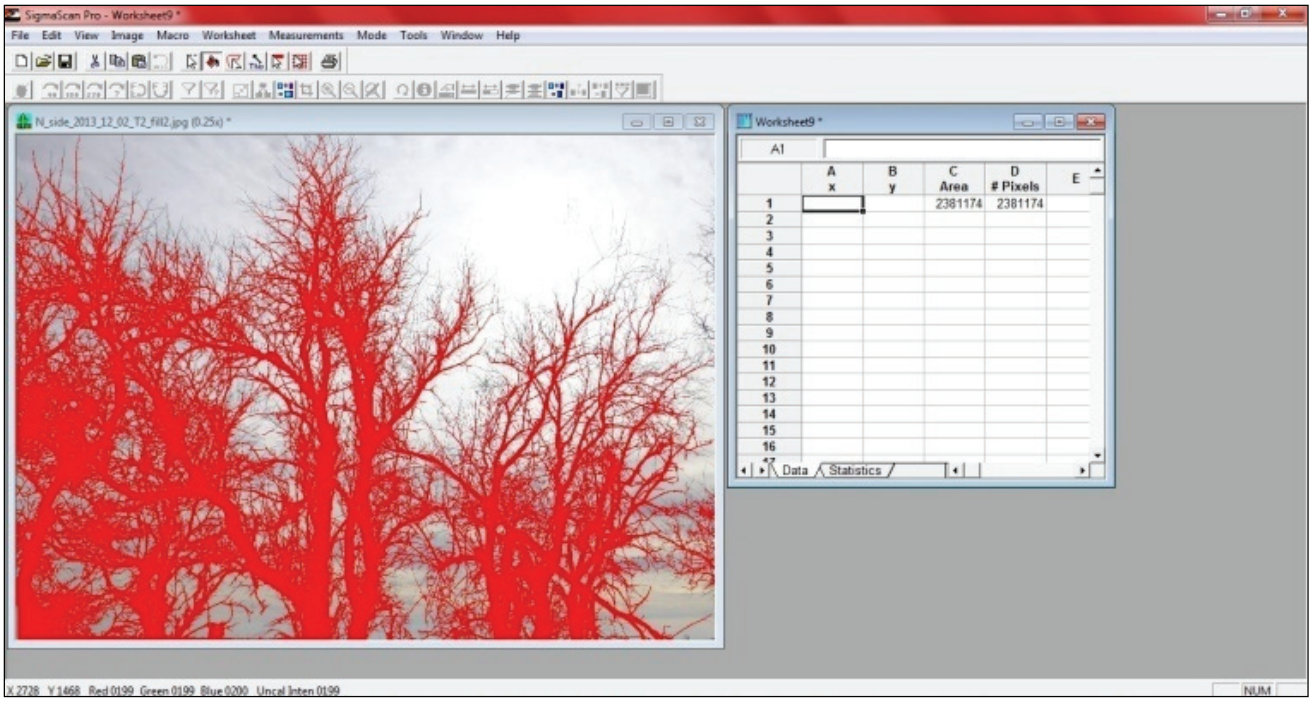

(a)

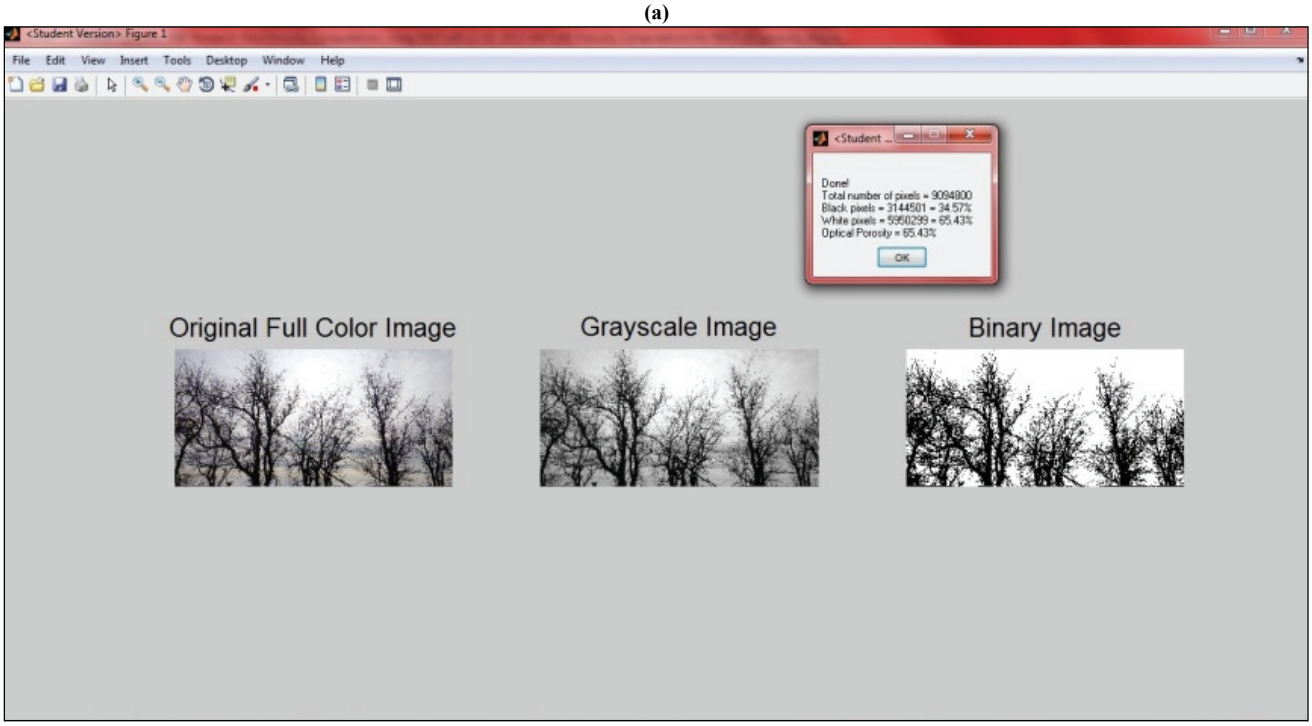

(b)

Figure 4. Optical porosity determination using (a) SigmaScan Pro and (b) MATLAB.

$$D_b = \int_0^S \left[\left(\frac{1}{2\rho_{air} u_{up}^2} \right) - \left(\frac{1}{2\rho_{air} u_{down}^2} \right) \right] dz \qquad (5)$$

The drag coefficient values computed in this study were based on the drag forces calculated using leeward wind speeds at the 7*H* and 10*H* distances away from the barrier to obtain a valid assumption that pressure forces are negligible and that no end effects were present for the vegetative barrier (Hagen and Skidmore, 1971).

METEOROLOGICAL DATA

To monitor weather data at the site, a weather station (Vantage Pro2, Davis Instruments, Hayward, Cal.) was equipped with a solar panel and an integrated sensor suite consisting of temperature and humidity sensors, anemometer, and rain gauge. A weather-resistant shelter housed the electronic components within the sensor suite, which operated with solar power. A battery-operated wireless console gathered data from the weather station.

Data Analysis

Data for the wind profiles were screened, and wind speeds that corresponded to situations with stoppages of the cup anemometer (limited by a minimum of 2 m s^{-1}) were eliminated from analysis. Wind speed reductions were obtained from three replications of wind profiling tests at each cup anemometer height for each distance leeward from the barrier. For comparison of the two image analysis methods, optical porosities were obtained from three images at each location (north and south sides) for the leaf-on and leaf-off conditions; the section of the vegetative barrier used was the same transect used for the wind profile measurements. To compare porosities α_p and β_p, the original images used for the image analysis comparison were each divided horizontally into five sections corresponding to the heights at which the lower five anemometers (up to 8.2 m height) recorded wind speed data (a total of six anemometers were used during the field tests), and the optical porosities were computed individually for each of the sections. Computation of the drag coefficient was based on wind speed profiles at 7*H* and 10*H* distances for three replicates of each leaf condition. Mean values of wind speed, optical porosity, and drag coefficient were compared using the normality and homogeneity of variances assumption and a standard paired t-test in Microsoft Excel (Microsoft Corp., Redmond, Wash.). Analysis of variance (ANOVA) was used to determine the effects of vegetation density and height. A 5% level of significance was used for all cases. CurveExpert 1.4 (Hyams, 2013) was used to plot best-fit curves.

Results and Discussion

Wind Profile

Wind rose plots during the field tests for the leaf-on and leaf-off conditions are shown in figure 5. The percentages represent the amount of time that the wind blew from a specific direction, and the colors indicate the magnitude of wind speed. Tests were conducted with ample wind (3 to 7 m s^{-1}) to obtain wind profiles for the various distances away from the barrier for the two leaf conditions of the Osage orange barrier. During tests for the leaf-off condition, the wind direction and speed changed more than during the leaf-on condition. Wind speeds ranged from 6 to 7 m s^{-1} during the leaf-on condition and from 3 to 6 m s^{-1} during the leaf-off condition.

Figure 6 shows a comparison of normalized wind speeds between the two leaf conditions, demonstrating the effect of the Osage orange barrier on leeward wind speeds. Normalization was calculated by dividing the leeward wind speed (bleed wind speed, U_b) at specific heights with a paired windward wind speed at the same height. The plot shows the mean of three replications of wind profiles at various distances from the barrier; *xH* is the distance from the barrier at multiples of height *H*. Without leaves, a deciduous tree barrier, such as the Osage orange barrier, is able to lower the leeward wind speeds, although not as effectively as with leaves, as evidenced by the increased bleed wind speeds (U_b) with respect to the approach wind speeds ($U_{approach}$). In addition, leeward wind speeds recover faster (i.e., wind speed values are near windward values from 12*H* onward) for the leaf-off condition as compared to the leaf-on condition. In general, the Osage orange barrier effectively shelters leeward agricultural land beyond 10*H*, which is considered a common estimate of the sheltering effectiveness of vegetative barriers (Raine and Stevenson, 1977).

Wind speeds were measured at different heights and leeward distances perpendicular to the vegetative barrier, and the speed reductions are shown in figure 7 (leaf-on condition) and figure 8 (leaf-off condition). According to the wind profile of the Osage orange barrier with leaves (fig. 7), the

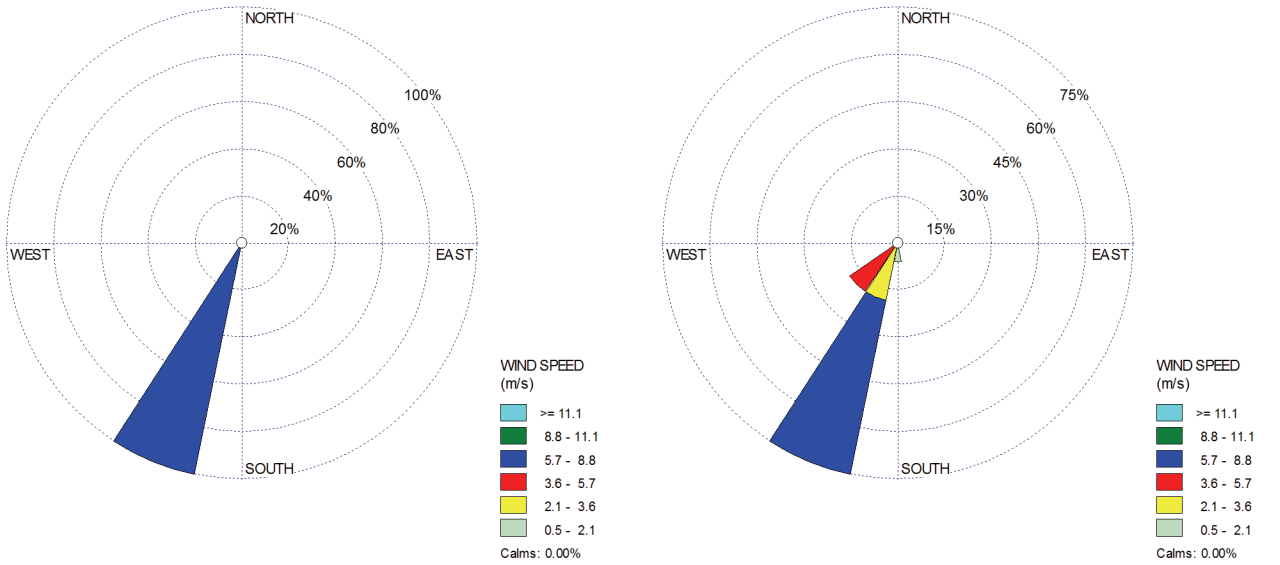

(a) (b)

Figure 5. Wind rose plots during field tests for (a) leaf-on and (b) leaf-off conditions of the Osage orange barrier. Concentric circles represent percentage of winds coming from the indicated direction within the specified wind speed range.

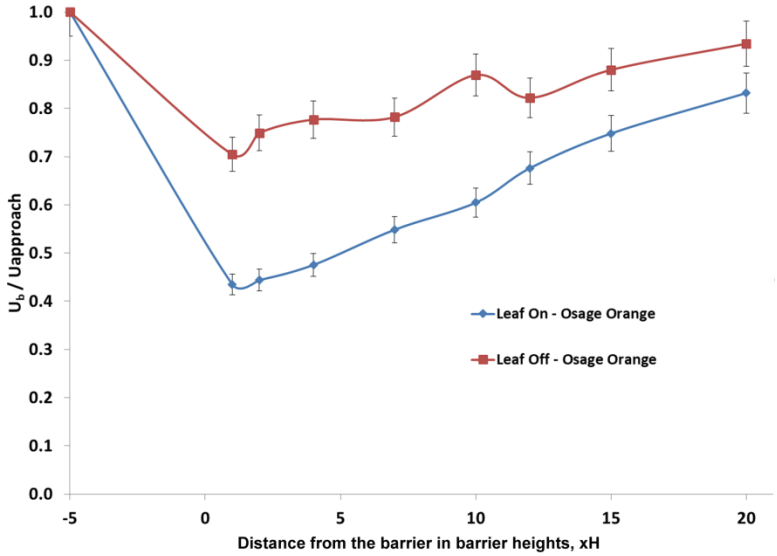

Figure 6. Comparison of normalized mean wind speeds between leaf-on and leaf-off conditions of the Osage orange barrier; *xH* is the distance from the barrier in multiples of mean tree height (*H* = 8.5 m). Each point represents the ratio of bleed wind speed (U_b) to approaching wind speed ($U_{approach}$) (mean 10 min speeds averaged over all heights). Vertical whiskers represent standard errors.

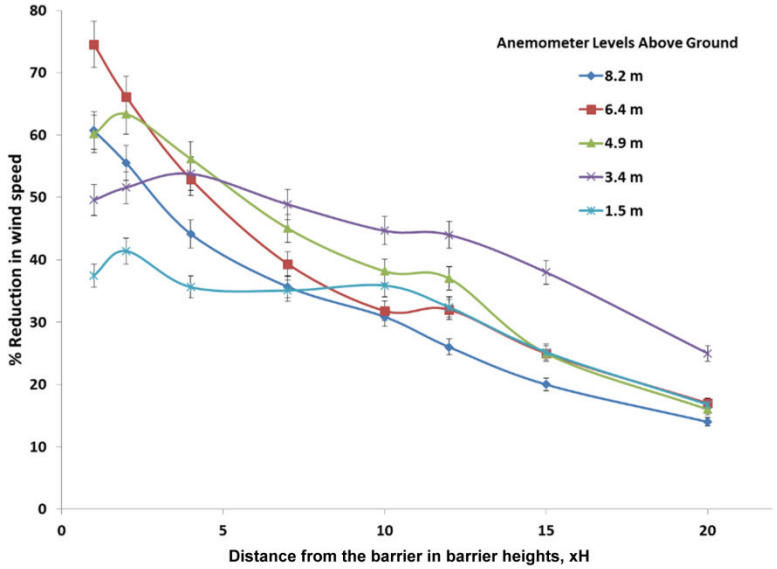

Figure 7. Percent reduction in wind speed leeward of the Osage orange barrier for the leaf-on condition; *xH* is the distance from the barrier in multiples of mean tree height (*H* = 8.5 m). Vertical whiskers represent standard errors.

reduction in wind speed occurred primarily in the middle (by height) part of the barrier at the crown (the portion of tree where leaves and branches extend from the trunk). This was expected because the presence of leaves provides more obstruction of airflow compared to the lower portions of the trees, where the trunks are located and gaps exist, thereby providing less reduction in the lower portion of the barrier. Figure 7 shows that, for the 1*H* distance from the barrier, the upper portion of the barrier (8.2 m above the ground, where the mean barrier height is 8.5 m) had lower wind speed reduction than the middle crown portion, potentially due to faster recovery of wind speed at that height because there were fewer leaves to retard airflow. The results for the leaf-on condition in this study are consistent with those reported by Woodruff et al. (1963). For example, the highest wind speed reduction by the Osage orange barrier was at a position close to the barrier. However, Woodruff et al. (1963) limited their measurements of the sheltering efficiency of an Osage orange barrier (mean height of 4.9 m) to the leaf-on condition only, with anemometer heights of 0.30, 0.61, and 1.22 m above the ground (≤1.22 m in representative heights), and they did not consider porosity or other factors that can affect sheltering efficiency.

For the leaf-off condition, figure 8 shows that the lower portions of the barrier reduced wind speeds leeward of the Osage orange barrier more than the upper portions. Even with leaves absent on the lower portions of the trees, the presence of larger branches and trunks provided significant reduction in wind speeds, especially close to the leeward side of the barrier, as compared to the upper portion of the barrier where thinner branches did not provide significant wind speed reduction with the leaves absent. Similar to figure 6,

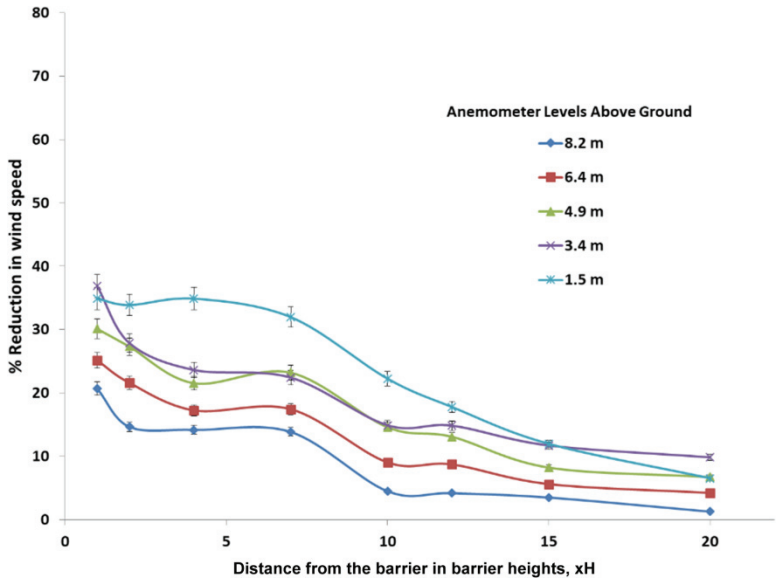

Figure 8. Percent reduction in wind speed leeward of the Osage orange barrier for the leaf-off condition; *xH* is the distance from the barrier in multiples of mean tree height (*H* = 8.5 m). Vertical whiskers represent standard errors.

faster re-establishment of the wind profile was achieved for the leaf-off condition because fewer elements (total leaves and branches) were present to hinder airflow and induce the formation of a recirculation zone behind the vegetative barrier (Schwartz et al., 1995).

POROSITY DETERMINATION

The two image analysis methods showed no significant difference ($p > 0.05$) with respect to the computed mean β_p of the Osage orange barrier for a specific leaf condition, but they showed significant differences ($p < 0.05$) between the two leaf conditions (leaf-on and leaf-off) (table 1). In addition, for both locations (north and south sides) where the images were taken, β_p did not show any significant difference ($p > 0.05$) for a specific leaf condition. Table 1 presents the overall means of measured β_p values based on image analysis over the full barrier height.

No significant difference ($p > 0.05$) was observed for measured values between the grayscale (MATLAB) and color (SigmaScan Pro) analysis methods. However, the β_p values computed using binary images were generally greater than those of the color analysis method. Visual comparisons showed that the binary images produced by the grayscale method did not include portions of the barrier seen in the original images, especially small branches and leaves that were part of the foreground. The color analysis method allowed adjustable separation of the image background and foreground by filling every pixel based on the desired RGB color value. Based on these differences, the β_p values based on the color analysis method were selected for use.

Table 1. Comparison of means and standard errors of the mean (SEM) of optical porosity (β_p) obtained using grayscale and color analyses.[a]

Image	Grayscale	Color
Leaf-on north side	27.2 ±1.0 Aa	23.1 ±1.6 Aa
Leaf-off north side	64.0 ±1.0 Ba	63.0 ±1.6 Ba
Leaf-on south side	28.4 ±0.5 Aa	22.5 ±0.7 Aa
Leaf-off south side	59.9 ±1.1 Ba	58.2 ±1.0 Ba

[a] Different uppercase letters (A,B) between rows and different lowercase letters (a,b) between columns indicate significant differences ($p < 0.05$). Means were derived from three images on each side of the same section of the barrier (the same transect used for wind profile measurements).

The relationship between α_p and β_p is shown in figure 9. The curve-fit results ($\alpha_p = \beta_p^{0.65}$, $R^2 = 0.78$) show a good correlation between values of α_p calculated using wind profiles from the leaf-on and leaf-off conditions of the Osage orange barrier with values of β_p calculated using color image analysis. During the curve-fit tests, the empirical equation obtained by Guan et al. (2003), $\alpha_p = \beta_p^{0.4}$, was found to differ slightly from the empirical equation obtained in this study. An exponent of 0.65 rather than 0.4 was found to be a better fit for the Osage orange barrier. The difference could be attributed to the type of measurement. Guan et al. (2003) used a wind tunnel with highly controlled conditions, while our study used full-scale tests in a field setting with variable winds. In addition, a real vegetative barrier was used for our study, compared to the artificial custom model used by Guan

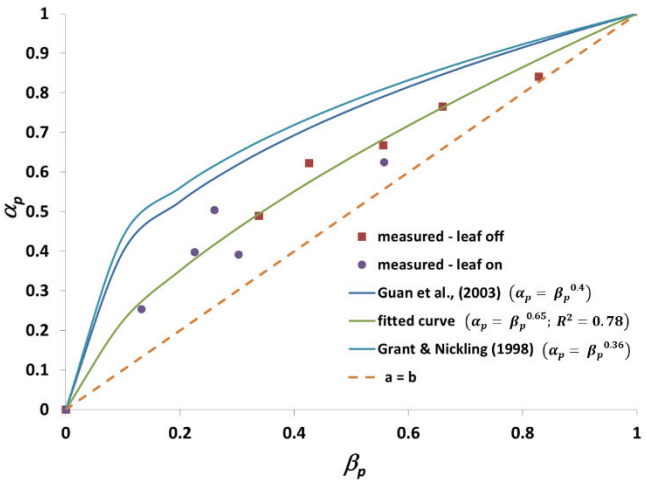

Figure 9. Relationship between measured aerodynamic (α_p) and optical (β_p) porosities of Osage orange barrier. The data points represent mean aerodynamic porosities based on mean wind speeds (10 min average over all anemometer heights) or mean optical porosities over the full barrier height.

et al. (2003) and the artificial Christmas tree used by Grant and Nickling (1998). As Grant and Nickling (1998) stated, the exponent for the empirical equation depends on the composition of the leaves and the breadth:width ratio of the vegetative barrier. Our study showed that the methodology of Guan et al. (2003) can be applied in a field setting as long as the field conditions are suitable for obtaining wind profiles, i.e., winds not too strong nor too calm and within 6 to 12 m s^{-1}, similar to the experiment reported by Hagen and Skidmore (1971). The images used for β_p determination should be taken during calm winds, according to Loeffler (1992) and Kenney (1987), to prevent excessive movement of leaves and branches, which creates varying gaps in the barrier and potentially leads to inconsistent β_p readings.

The scatter of the points in figure 9 for the leaf-on and leaf-off conditions could be a result of the difficulties encountered during the field tests. This study was limited by the availability of anemometers, so multiple vertical gradient measurements of wind speed were not taken at various locations parallel to the vegetative barrier. During the experiment, only a single transect relative to a section of the barrier strip was used, and wind speeds at various distances from the barrier and at various vertical gradients were collected to obtain the aerodynamic parameters. However, even if multiple measurements were taken simultaneously across the width of the barrier at various vertical gradients, acquisition of representative values for α_p would be difficult because of the temporal variability in wind speeds windward of the barrier, especially during field experiments during leaf-off conditions, as evidenced by the wind rose plot (fig. 5). In addition, the presence of holes and gaps in the barrier at locations of expected increased bleed wind speed (as observed by Guan et al., 2003) and the structural complexity of the barrier during the leaf-on condition, with the movement of leaves and branches, causes changes in leeward wind speeds. As such, the movement of leaves and branches complicates the measurement of leeward profiles close to the barrier that are necessary to compute the value of α_p.

Vegetative Barrier Drag Coefficient

Figure 10 shows a comparison of C_D values between the leaf-on and leaf-off conditions of the Osage orange barrier based on the methodology of Hagen and Skidmore (1971). During the field measurements, wind speeds varied from 4 m s^{-1} to approximately 7 m s^{-1}, similar to the tests reported by Hagen and Skidmore (1971) and Meroney (1968). Drag coefficients were independent of wind speed, especially for wind speeds less than 6 to 8 m s^{-1}. The expected C_D values, based on Hagen and Skidmore (1971), for a given porosity were close to the C_D values pertaining to specific β_p values of the Osage orange barrier (as shown by $R^2 = 0.98$). Despite marked differences between rigid vegetative barriers and trees, which have continuously moving leaves and branches during field tests, the obtained C_D values were similar over the range of wind speeds tested.

The trend of decreasing C_D with increasing vegetative barrier porosity may be due to changes in wind momentum as the wind encounters the vegetative barrier and flows continuously to the leeward side of the barrier. Schwartz et al. (1995) detailed what happens behind various types of model vegetative barriers; they found that some portions had recirculation zones leeward of the barrier, while others did not. These recirculation zones could cause large eddies immediately leeward of the barrier, greatly affecting the wind behavior behind the barrier. The presence of gaps or holes within the barrier cause jetting of air through the barrier, which also forms eddies behind the barrier. Windward of the barrier, the loss of air momentum is caused by the presence of vegetative elements (leaves, branches, and trunks) during the leaf-on condition of the barrier, consequently amplifying the multiple transfers of momentum among elements within the barrier (Grant and Nickling, 1998), especially at the crown portion of Osage orange trees. The crown portion of the trees was found to be responsible for much of the wind speed reduction by obstructing the airflow, effectively sheltering the leeward area. As such, the larger the crown portion, the larger the area that is sheltered leeward of the bar-

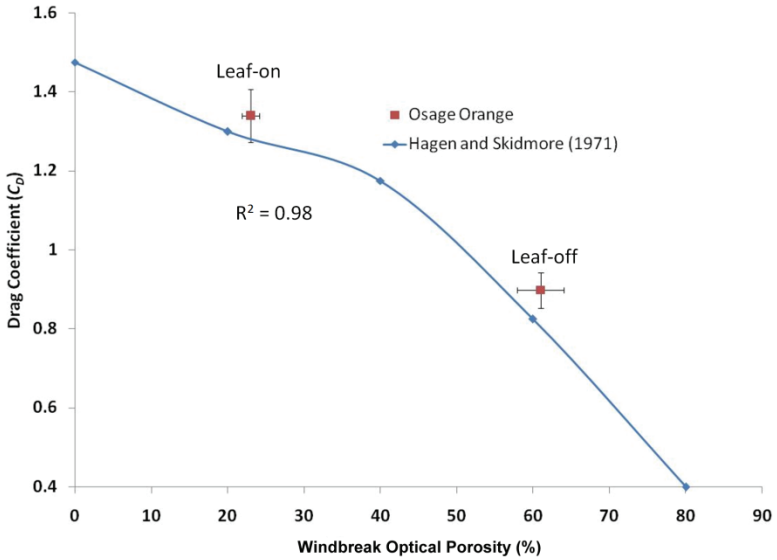

Figure 10. Comparison of drag coefficient versus optical porosity, where the Osage orange data points represent mean values for the leaf-on and leaf-off conditions. Means were taken as the average of all wind speeds for each leaf condition. Whiskers represent standard errors. The R^2 value represents the correlation of measured values in this study with the data of Hagen and Skidmore (1971).

rier. The momentum transfer creates a barrier resistance to airflow that causes the drag coefficient to increase. When the leaves fall off, the porosity increases, resulting in a decrease in the drag coefficient.

CONCLUSIONS

Deciduous trees, such as Osage orange, are commonly used as vegetative barriers in Kansas. The aerodynamic (α_p) and optical (β_p) porosities of this tree species were estimated using wind profiles and image analysis, respectively, and an empirical equation relating the two porosities was developed ($\alpha_p = \beta_p^{0.65}$, $R^2 = 0.78$). Vertical wind profiles were also used to estimate the drag coefficient, which determined how much resistance the barrier offered to incoming airflow to protect the land leeward of the barrier during leaf-on and leaf-off conditions of the trees. As expected, the leaf-on condition showed lower porosity and greater drag coefficient values compared to the leaf-off condition. Thus, the leaf condition is a good indicator of the drag coefficient and porosity of a specific vegetative barrier. A strong correlation between optical porosity and drag coefficient was observed (R^2 = 0.98).

The aerodynamic parameters (porosities and drag coefficients) obtained in this study could be useful for validating numerical simulations for further optimization of the sheltering efficiency of vegetative barriers. This first effort to quantify the aerodynamic parameters of an Osage orange barrier could be extended in future work by (1) simultaneously measuring all wind speeds perpendicular to the barrier and (2) evaluating the transition period, i.e., when the leaves of these deciduous trees have partially fallen off, to obtain measurements of optical porosity and drag as a function of leaf density.

ACKNOWLEDGEMENTS

Technical assistance provided by Matthew Kucharski, Dennis Tilley, Hubert Lagae, Neil Baker, and Chris Shultz is acknowledged.

REFERENCES

Billman Stunder, B. J., & Arya, S. P. S. (1988). Windbreak effectiveness for storage pile fugitive dust control: A wind tunnel study. *J. Air Pollut. Control. Assoc., 38*(2), 135-143. https://doi.org/10.1080/08940630.1988.10466360

Bird, P. R., Bicknell, D., Bulman, P. A., Burke, S. J., Leys, J. F., Parker, J. N., ... Voller, P. (1992). The role of shelter in Australia for protecting soils, plants, and livestock. *Agroforestry Syst., 20*(1), 59-86. https://doi.org/10.1007/bf00055305

Bitog, J. P., Lee, I. B., Hwang, H. S., Shin, M. H., Hong, S. W., Seo, I. H., ... Pang, Z. (2011). A wind tunnel study on aerodynamic porosity and windbreak drag. *Forest Sci. Tech., 7*(1), 8-16. https://doi.org/10.1080/21580103.2011.559939

Bouvet, T., Loubet, B., Wilson, J. D., & Tuzet, A. (2007). Filtering of windborne particles by a natural windbreak. *Boundary-Layer Meteorol., 123*(3), 481-509. https://doi.org/10.1007/s10546-007-9156-y

Brandle, J. R., Hodges, L., & Zhou, X. H. (2004). Windbreaks in North American agricultural systems. *Agroforestry Syst., 61*(1), 65-78. https://doi.org/10.1023/b:agfo.0000028990.31801.62

Burel, F., & Baudry, J. (1995). Social, aesthetic, and ecological aspects of hedgerows in rural landscapes as a framework for greenways. *Landscape Urban Plan., 33*(1), 327-340. https://doi.org/10.1016/0169-2046(94)02026-C

Campi, P., Palumbo, A. D., & Mastrorilli, M. (2009). Effects of tree windbreak on microclimate and wheat productivity in a Mediterranean environment. *European J. Agron., 30*(3), 220-227. https://doi.org/10.1016/j.eja.2008.10.004

Cleugh, H. A. (1998). Effects of windbreaks on airflow, microclimates, and crop yields. *Agroforestry Syst., 41*(1), 55-84. https://doi.org/10.1023/a:1006019805109

Cornelis, W. M., & Gabriels, D. (2005). Optimal windbreak design for wind-erosion control. *J. Arid Environ., 61*(2), 315-332. https://doi.org/10.1016/j.jaridenv.2004.10.005

Cullen, S. (2005). Trees and wind: A practical consideration of the drag equation velocity exponent for urban tree risk management. *J. Arboricult., 31*(3), 101-113.

Ffolliott, P. (1998). Multiple benefits of arid land agroforestry home gardens and riparian ecosystems. In S. J. Josiah (Ed.), *Proc. Conf. Enterprise Development through Agroforestry: Farming the Forest for Specialty Products* (pp. 41-46). Minneapolis, MN: University of Minnesota, Center for Integrated Natural Resources and Agricultural Management.

Grala, R. K., Tyndall, J. C., & Mize, C. W. (2010). Impact of field windbreaks on visual appearance of agricultural lands. *Agroforestry Syst., 80*(3), 411-422. https://doi.org/10.1007/s10457-010-9335-6

Grant, P. F., & Nickling, W. G. (1998). Direct field measurement of wind drag on vegetation for application to windbreak design and modeling. *Land Degrad. Devel., 9*(1), 57-66. https://doi.org/10.1002/(SICI)1099-145X(199801/02)9:1<57::AID-LDR288>3.0.CO;2-7

Gregory, N. G. (1995). The role of shelterbelts in protecting livestock: A review. *New Zealand J. Agric. Res., 38*(4), 423-450. https://doi.org/10.1080/00288233.1995.9513146

Guan, D., Zhang, Y., & Zhu, T. (2003). A wind-tunnel study of windbreak drag. *Agric. Forest Meteorol., 118*(1), 75-84. https://doi.org/10.1016/S0168-1923(03)00069-8

Hagen, L. J., & Skidmore, E. L. (1971). Windbreak drag as influenced by porosity. *Trans. ASAE, 14*(3), 464-465. https://doi.org/10.13031/2013.38315

Heisler, G. M., & Dewalle, D. R. (1988). 2. Effects of windbreak structure on wind flow. *Agric. Ecosyst. Environ., 22-23*, 41-69. https://doi.org/10.1016/0167-8809(88)90007-2

Hyams, D. G. (2013). CurveExpert 1.4. Hyams Development. Retrieved from www.curveexpert.net

Kenney, W. A. (1987). A method for estimating windbreak porosity using digitized photographic silhouettes. *Agric. Forest Meteorol., 39*(2), 91-94. https://doi.org/10.1016/0168-1923(87)90028-1

Koh, I., Park, C.-R., Kang, W., & Lee, D. (2014). Seasonal effectiveness of a Korean traditional deciduous windbreak in reducing wind speed. *J. Ecol. Environ., 37*(2), 91-97. https://doi.org/10.5141/ecoenv.2014.011

Koizumi, A., Motoyama, J.-i., Sawata, K., Sasaki, Y., & Hirai, T. (2010). Evaluation of drag coefficients of poplar-tree crowns by a field test method. *J. Wood Sci., 56*(3), 189-193. https://doi.org/10.1007/s10086-009-1091-8

Kort, J. (1988). 9. Benefits of windbreaks to field and forage crops. *Agric. Ecosyst. Environ., 22-23*, 165-190. https://doi.org/10.1016/0167-8809(88)90017-5

Kozmar, H., Procino, L., Borsani, A., & Bartoli, G. (2012). Sheltering efficiency of wind barriers on bridges. *J. Wind Eng. Ind. Aerodyn., 107-108*, 274-284. https://doi.org/10.1016/j.jweia.2012.04.027

Loeffler, A. E., Gordon, A. M., & Gillespie, T. J. (1992). Optical

porosity and windspeed reduction by coniferous windbreaks in southern Ontario. *Agroforestry Syst., 17*(2), 119-133.
Mader, T. L., Dahlquist, J. M., Hahn, G. L., & Gaughan, J. B. (1999). Shade and wind barrier effects on summertime feedlot cattle performance. *J. Animal Sci., 77*(8), 2065-2072. https://doi.org/10.2527/1999.7782065x
Meroney, R. N. (1968). Characteristics of wind and turbulence in and above model forests. *J. Appl. Meteorol., 7*(5), 780-788. https://doi.org/10.1175/1520-0450(1968)007<0780:cowati>2.0.co;2
Raine, J. K., & Stevenson, D. C. (1977). Wind protection by model fences in a simulated atmospheric boundary layer. *J. Wind Eng. Ind. Aerodyn., 2*(2), 159-180. https://doi.org/10.1016/0167-6105(77)90015-0
Schwartz, R. C., Fryrear, D. W., Harris, B. L., Bilbro, J. D., & Juo, A. S. (1995). Mean flow and shear stress distributions as influenced by vegetative windbreak structure. *Agric. Forest Meteorol., 75*(1), 1-22. https://doi.org/10.1016/0168-1923(94)02206-Y
Sellier, D., Brunet, Y., & Fourcaud, T. (2008). A numerical model of tree aerodynamic response to a turbulent airflow. *Forestry , 81*(3), 279-297. https://doi.org/10.1093/forestry/cpn024
Steffens, J. T., Wang, Y. J., & Zhang, K. M. (2012). Exploration of effects of a vegetation barrier on particle size distributions in a near-road environment. *Atmos. Environ., 50*, 120-128. https://doi.org/10.1016/j.atmosenv.2011.12.051
Stredova, H., Podhrazska, J., Litschmann, T., Streda, T., & Roznovsky, J. (2012). Aerodynamic parameters of windbreak based on its optical porosity. *Contrib. Geophys. Geodesy, 42*(3), 213-226.
Sudhishri, S., Dass, A., & Lenka, N. K. (2008). Efficacy of vegetative barriers for rehabilitation of degraded hill slopes in eastern India. *Soil Tillage Res., 99*(1), 98-107. https://doi.org/10.1016/j.still.2008.01.004
Sudmeyer, R. A., Crawford, M. C., Meinke, H., Poulton, P. L., & Robertson, M. J. (2002). Effect of artificial wind shelters on the growth and yield of rainfed crops. *Australian J. Exp. Agric., 42*(6), 841-858. https://doi.org/10.1071/EA02018
Sun, D., & Dickinson, G. R. (1997). Early growth of six native Australian tree species in windbreaks and their effect on potato growth in tropical northern Australia. *Forest Ecol. Mgmt., 95*(1), 21-34. https://doi.org/10.1016/S0378-1127(97)00005-4
Vigiak, O., Sterk, G., Warren, A., & Hagen, L. J. (2003). Spatial modeling of wind speed around windbreaks. *Catena, 52*(3), 273-288. https://doi.org/10.1016/S0341-8162(03)00018-3
Wang, H., & Takle, E. S. (1996). On three-dimensionality of shelterbelt structure and its influences on shelter effects. *Boundary-Layer Meteorol., 79*(1), 83-105. https://doi.org/10.1007/bf00120076
Wilson, J. D. (1987). On the choice of a windbreak porosity profile. *Boundary-Layer Meteorol., 38*(1), 37-49. https://doi.org/10.1007/bf00121553
Wilson, J. D. (2005). Deposition of particles to a thin windbreak: The effect of a gap. *Atmos. Environ., 39*(30), 5525-5531. https://doi.org/10.1016/j.atmosenv.2005.06.006
Woodruff, N. P., Fryrear, D. W., & Lyles, L. (1963). Engineering similitude and momentum transfer principles applied to shelterbelt studies. *Trans. ASAE, 6*(1), 41-47. https://doi.org/10.13031/2013.40822
Zhu, J. J. (2008). Wind shelterbelts. In B. D. Fath (Ed.), *Encyclopedia of ecology* (pp. 3803-3812). Oxford, UK: Academic Press. https://doi.org/10.1016/B978-008045405-4.00366-9